Journal of Molecular Structure 1036 (2013) 439–446

Contents lists available at SciVerse ScienceDirect

Journal of Molecular Structure

journal homepage: www.elsevier.com/locate/molstruc

Halogen substituted quinolylsalicylaldimines: Four halogens three structural types

Jitnapa Sirirak [a], Wasinee Phonsri [a], David J. Harding [a,*], Phimphaka Harding [a], Pimonrat Phommon [b], Wannapa Chaoprasa [b], Rebecca M. Hendry [c], Thomas M. Roseveare [c], Harry Adams [c]

[a] Molecular Technology Research Unit Cell, Walailak University, Thasala, Nakhon Si Thammarat 80161, Thailand
[b] Department of Chemistry, Faculty of Science, Naresuan University, Phitsanulok 65000, Thailand
[c] Department of Chemistry, University of Sheffield, Sheffield S3 7HF, United Kingdom

HIGHLIGHTS

- The structures of four halogen substituted quinolylsalicylaldimines are reported.
- The structures exhibit hydrogen bonds, π–π and C—H···N/O interactions.
- The chloro derivative features an unexpected 'inverted' conformation.
- The conformation determines the strength of the hydrogen bond.
- DFT calculations indicate conformational preferences are halogen dependent.

ARTICLE INFO

Article history:
Received 18 October 2012
Received in revised form 12 November 2012
Accepted 12 November 2012
Available online 23 November 2012

Keywords:
Salicylaldimines
π–π Stacking
Hydrogen bonding
DFT calculations

ABSTRACT

A series of halogen substituted 5-X-*N*-(8-quinolyl)salicylaldimines (Hqsal^X, X = F **1**, Cl **2**, Br **3** and I **4**) have been prepared, characterized and the crystal structures of all four are reported. The compounds form stacks, in most cases held together either by π–π or lone pair(N)–π interactions. All compounds exhibit an *intramolecular* O—H···N hydrogen bond with **2** also displaying an *intermolecular* O—H···O hydrogen bonding square. Additional C—H···N/O and C—H···π interactions serve to link neighbouring Hqsal^X molecules with **3** and **4** forming narcissistic dimers. While the halogen has a profound effect on the structure it is not involved in either hydrogen or halogen bonding in any of the structures. DFT calculations suggest that the conformational preference is dependent on the halogen.

1. Introduction

The construction and design of molecules which crystallize in a predictable manner leading to expected structures remains the ultimate goal of crystal engineering [1,2]. One of the reasons why it is so difficult to predict a crystal structure based purely on the molecular structure relates to the interplay between the various interactions that in turn determine which structure is the most stable [3–10]. It follows that understanding how different interactions combine to form a complete structure and which are the structure determining interactions is vital if some degree of predictability is to be achieved [11].

To do this requires utilization and understanding of a wide range of supramolecular interactions including classical hydrogen bonds [3,4], weak hydrogen bonds (e.g. C—H···N/O interactions) [5,6] and π–π interactions [8,9]. A more recent addition to the aforementioned interactions is halogen bonding [12–15]. Halogen bonds are weak supramolecular non-covalent interactions and are often similar to hydrogen bonds where the hydrogen is replaced by a halogen which acts as a halogen bond donor and are attributed to electrostatic forces. The halocarbons can effectively be the electropositive site that can interact with an electron donating atom/group to produce higher dimensional structures. However, they may also function as halogen bond acceptors forming C—X···N/O interactions as well as halogen–halogen interactions [16–19]. This flexibility is associated with the polarizability of the halogens which have a positive σ-hole along the C—X axis and belt of negative charge perpendicular to this C—X bond [20]. The more polarizable the halogen the stronger the interaction will be, consequently halogen bonding typically increases on moving from F to I.

Halogen bond strength can possibly be tuned by modifying the substituents on the carbon skeleton [21]. Our attention was drawn to the halogen substituted 5-X-*N*-(8-quinolyl)salicylaldimines (Hqsal^X, X = F, Cl, Br and I) [22,23] as these contain two different

* Corresponding author. Tel./fax: +66 75 672004.
E-mail address: hdavid@wu.ac.th (D.J. Harding).

0022-2860/$ - see front matter © 2012 Elsevier B.V. All rights reserved.
http://dx.doi.org/10.1016/j.molstruc.2012.11.028

Table 1
Crystallographic data and structure refinement for **1**–**4**.

	1	2	3	4
Formula	$C_{16}H_{11}FN_2O$	$C_{16}H_{11}ClN_2O$	$C_{16}H_{11}BrN_2O$	$C_{16}H_{11}IN_2O$
Molecular weight ($g\,mol^{-1}$)	266.27	282.72	327.18	374.17
Crystal system	Monoclinic	Monoclinic	Monoclinic	Monoclinic
Space group	$P2_1/c$	$P2_1/c$	$P2_1/n$	$P2_1/c$
a (Å)	10.0551(5)	13.4764(14)	16.4841(3)	17.014(4)
b (Å)	9.2429(4)	3.7721(4)	4.68910(10)	4.6068(10)
c (Å)	14.1107(7)	25.991(2)	17.1739(3)	17.418(4)
α (°)	90	90	90	90
β (°)	104.421(2)	104.802(7)	99.7460(10)	99.835(4)
γ (°)	90	90	90	90
T (K)	293(2)	100(2)	100(2)	150(2)
Cell volume (Å^3)	1270.10(10)	1277.4(2)	1308.31(4)	1345.1(5)
Z	4	4	4	4
Absorption coefficient (mm^{-1})	0.099	0.295	3.138	2.377
Reflections collected	16663	6562	13316	11812
Independent reflections, R_{int}	3413, 0.027	2267, 0.055	3033, 0.026	3083, 0.055
Max. and min. transmission	0.9882 and 0.9795	0.9740 and 0.8963	0.5726 and 0.4064	0.7800 and 0.5168
Restraints/parameters	0/182	0/181	0/181	0/182
Final R indices [$I > 2\sigma(I)$]: R_1, wR_2	0.0492, 0.1476	0.0391, 0.1416	0.0246, 0.0767	0.0447, 0.1194

types of aromatic rings, a hydroxyl group as well as the halogens and may be expected to also engage in hydrogen bonding, C—H···π and π–π interactions in addition to any halogen bonds. In examining this series, we hope to develop a better understanding of the interplay between the various types of interactions and which dominate or cooperate with each other in such structures. Thus, in this work we report the crystal structures of all four compounds, explore the different structural motifs present and determine what affect the different halogens have on the extended structures in this apparently simple series.

2. Experimental

2.1. General remarks

All reactions were conducted in air using reagent grade solvents. All other chemicals were purchased from Sigma–Aldrich Chemical Company and used as received. Infrared spectra (as KBr discs) were recorded on a Perkin–Elmer Spectrum One infrared spectrophotometer in the range 400–4000 cm^{-1}. Electronic spectra were recorded in CH_2Cl_2 on a Shimadzu 1800 UV–Visible spectrometer. Elemental analyses were carried out on a Eurovector EA3000 analyser. ESI–MS were carried out on a Bruker Daltonics 7.0T Apex 4 FTICR Mass Spectrometer.

2.2. X-ray crystallography

Crystal data processing parameters for the structures of **1**–**4** are given in Table 1. X-ray quality crystals of **1**–**4** were grown by slow evaporation of a diisopropyl solution of Hqsal^X. Crystals were mounted on a glass fibre using perfluoropolyether oil and cooled rapidly to 150 or 100 K in a stream of cold nitrogen. In the case of **1** the structure was determined at 293 K. All diffraction data were collected on a Bruker APEXII area detector with graphite monochromated Mo Kα (λ = 0.71073 Å) [24]. After data collection, in each case an empirical absorption correction (SADABS) was applied [25], and the structures were then solved by direct methods and refined on all F^2 data using the SHELX suite of programs [26]. In all cases non-hydrogen atoms were refined with anisotropic thermal parameters; hydrogen atoms were included in calculated positions and refined with isotropic thermal parameters which were ca. 1.2 times the carbon atoms. The exception were the hydroxyl hydrogens which were located by low-theta difference Fourier and then refined with isotropic thermal parameters 1.5 times those of the oxygen atoms to which they are attached. All pictures were generated using the POV-Ray interface in X-SEED [27,28].

2.3. Synthesis of 5-fluoro-N-(8-quinolyl)salicylaldimine Hqsal^F

5-Fluorosalicylaldehyde (0.701 g, 5 mmol) was dissolved in diisopropyl ether (20 ml) giving a pale yellow solution. 8-Aminoquinoline (0.721 g, 5 mmol) was added and the solution stirred for 4 h giving an orange solution. Slow evaporation of the solution to ca. 5 ml gave orange crystals which were isolated by filtration, 1.22 g (92%). ν_{max}(KBr)/cm^{-1} 3435 (ν_{OH}), 3036, 2970 (ν_{CH}), 1613 ($\nu_{C=N}$). ^{1}H NMR ($CDCl_3$, 295 K; δ; ppm) 13.67 (OH), 8.99 (dd, 1H$_a$, J_{HH} 1.8, 4.2), 8.91 (s, 1H$_g$), 8.20 (dd, 1H$_c$, J_{HH} 1.8, 8.4), 7.75 (dd, 1H$_d$ J_{HH} 1.5, 8.1), 7.45–7.61 (m, 3H$_{b,e,f}$), 7.13 (m, 2H$_{h,j}$), 7.02 (dd, 1H$_i$, J_{HH} 4.2, 8.7). λ_{max}(CH_2Cl_2)/nm (ε, $dm^3\,mol^{-1}cm^{-1}$) 360 (48,000). m/z (ESI) 266 [M]$^+$. Calcd. for (found%) $C_{16}H_{11}FN_2O$: C, 72.16 (72.33); H, 4.16 (4.36); N, 10.53% (10.81).

2.4. Synthesis of 5-chloro-N-(8-quinolyl)salicylaldimine Hqsal^{Cl}

Hqsal^{Cl} was prepared in an analogous manner to Hqsal^F, orange/red microcrystals, 78%. ν_{max}(KBr)/cm^{-1} 3436 (ν_{OH}), 3042, 2994 (ν_{CH}), 1624 ($\nu_{C=N}$). ^{1}H NMR ($CDCl_3$, 295 K; δ; ppm) 13.96 (OH), 8.98 (s, 1H$_g$), 8.91 (s, 1H$_a$), 8.19 (dd, 1H$_c$, J_{HH} 8.1), 7.74 (s, 1H$_h$), 7.60 (m, 4H$_{b,d,e,f}$), 7.04 (s, 1H$_i$), 7.01 (s, 1H$_j$). λ_{max}(CH_2Cl_2)/nm (ε, $dm^3\,mol^{-1}cm^{-1}$) 359 (65,500). m/z (ESI) 282 [M]$^+$. Calcd. for (found%) $C_{16}H_{11}ClN_2O$: C, 67.96 (68.22); H, 3.92 (3.87); N, 9.91% (10.04).

2.5. Synthesis of 5-bromo-N-(8-quinolyl)salicylaldimine Hqsal^{Br}

Hqsal^{Br} was prepared in an analogous manner to Hqsal^F, red microcrystals, 88%. ν_{max}(KBr)/cm^{-1} 3369 (ν_{OH}), 3049, 2968 (ν_{CH}), 1617 ($\nu_{C=N}$). ^{1}H NMR ($CDCl_3$, 295 K; δ; ppm) 14.01 (OH), 8.99 (d, 1H$_a$, J_{HH} 4.2), 8.91 (s, 1H$_g$), 8.21 (d, 1H$_c$, J_{HH} 8.4), 7.75 (d, 1H$_d$ J_{HH} 8.1), 7.45–7.59 (m, 5H$_{b,e,f,h,j}$), 6.97 (d, 1H$_i$, J_{HH} 8.7). λ_{max}(CH_2Cl_2)/

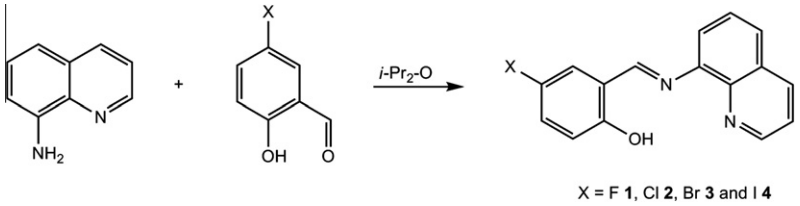

Scheme 1. Synthesis of Hqsal^X.

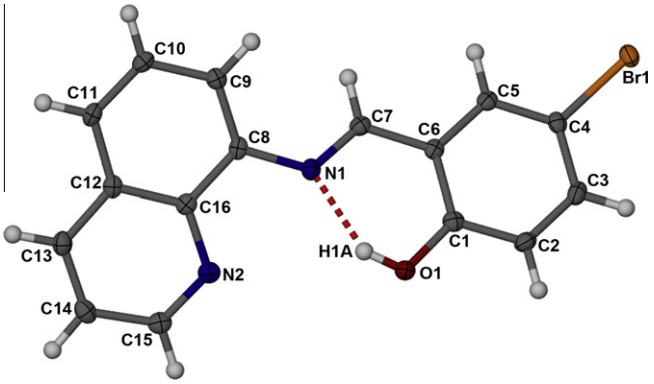

Fig. 1. POVRAY drawing of **3** with ellipsoids drawn at 50% probability showing the intramolecular hydrogen bond.

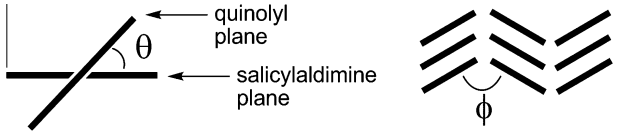

Fig. 2. Diagrammatic representation of the angles, θ and ϕ.

Table 2
Packing parameters for the Hqsal^{X} ligands.

	θ (°)[a]	ϕ (°)[b]	π–π
Hqsal^{F} **1**	14.7	89.7	3.88
Hqsal^{Cl} **2**	133.7	133.7	3.77
Hqsal^{Br} **3**	22.6	81.3	–
Hqsal^{I} **4**	5.1	86.9	–

[a] θ represents the angle between the quinolyl and salicylaldimine moiety.
[b] ϕ represents the angle between neighbouring Hqsal^{X} molecules.

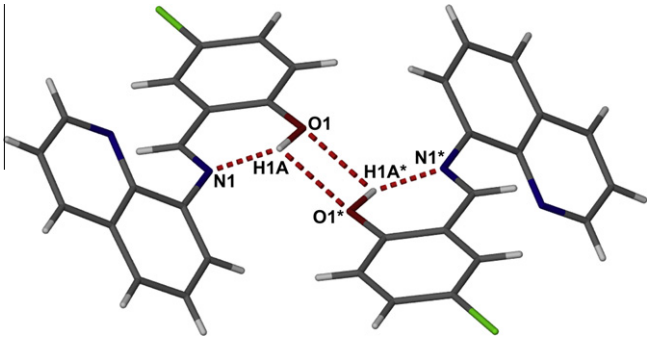

Fig. 3. POVRAY drawing showing the hydrogen bonding square in **2** (*symmetry code = 1−*x*, −*y*, 2 − *z*).

nm (ε, dm^3 mol^{-1}cm^{-1}) 350 (57,300). *m*/*z* (ESI) 326 [M]$^+$. Calcd. for (found%) $C_{16}H_{11}BrN_2O$: C, 58.72 (58.60); H, 3.39 (3.56); N, 8.56% (8.93).

2.6. Synthesis of 5-iodo-N-(8-quinolyl)salicylaldimine Hqsal^{I}

Hqsal^{I} was prepared in an analogous manner to Hqsal^{F}, dark red microcrystals, 85%. ν_{max}(KBr)/cm^{-1} 3436 (ν_{OH}), 3052, 2966 (ν_{CH}), 1616 ($\nu_{C=N}$). ^{1}H NMR ($CDCl_3$, 295 K; δ; ppm) 14.05 (OH), 8.98 (s, 1H$_g$), 8.92 (s, 1H$_a$), 8.89 (s, 1H$_c$), 8.21 (s, 1H$_h$), 7.59 (m, 4H$_{b,d,e,f}$), 7.28 (d, 1H$_i$, J_{HH} 7.2), 6.88 (d, 1H$_j$). λ_{max}(CH_2Cl_2)/nm (ε, dm^3 mol^{-1} cm^{-1}) 338 (61,800). *m*/*z* (ESI) 374 [M]$^+$. Calcd. for (found%) $C_{16}H_{11}IN_2O$: C, 51.34 (51.46); H, 2.96 (3.15); N, 7.49% (7.69).

3. Results and discussion

3.1. Synthesis and basic characterization of Hqsal-X

The compounds 5-X-*N*-(8-quinolyl)salicylaldimines (Hqsal^{X}, X = F **1**, Cl **2**, Br **3** and I **4**) were prepared in a simple one step reaction involving addition of the appropriate substituted salicylaldehyde to 8-aminoquinoline in diisopropyl ether (see Scheme 1). Previous syntheses have always involved the use of EtOH but we found the products to be more difficult to crystallize from this solvent whereas orange microcrystalline products are formed from diisopropyl ether. It should be noted that Hqsal^{Cl} and Hqsal^{Br} have previously been synthesized but no experimental details or spectroscopic studies were reported and are included here in the interests of completeness [22,23].

The compounds have been characterized by IR, ^{1}H NMR and UV–Vis spectroscopy with IR spectroscopy showing an imine stretch between 1613 and 1624 cm^{-1} while the hydroxyl group is present at 3369–3436 cm^{-1} confirming the formation of **1**–**4**. ^{1}H NMR spectra were recorded in $CDCl_3$ and display a characteristic peak at 8.91 or 8.92 ppm for the imino proton while the hydroxyl proton is found to be strongly deshielded indicative of strong hydrogen bonding to the imino nitrogen atom. The aromatic protons are found in their expected positions and are similar to values reported for Hqsal [29]. The UV–Vis spectra of the Hqsal^{X} ligands were recorded in dichloromethane. The Hqsal^{X} ligands exhibit a single intense absorption between 338–360 nm, which by comparison with Hqsal have been assigned to a $\pi \rightarrow \pi^*$ transition [29].

3.2. Structural studies of Hqsal^{X}

Single crystals of all the compounds were grown by slow evaporation of a solution of Hqsal^{X} in diisopropyl ether. Most of the compounds crystallize in the monoclinic space group $P2_1/c$ while Hqsal^{Br} crystallizes in $P2_1/n$ as does the previously reported Hqsal and Hqsal^{OMe} [29,30]. Interestingly, despite this none of the compounds are isostructural though some contain the same structural motifs.

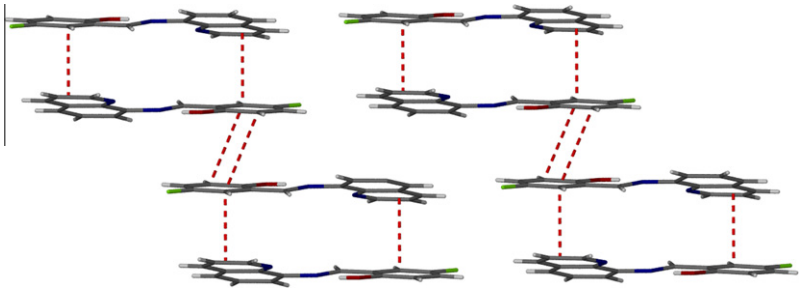

Fig. 4. π–π Interactions showing the dimers in the structure of **1**.

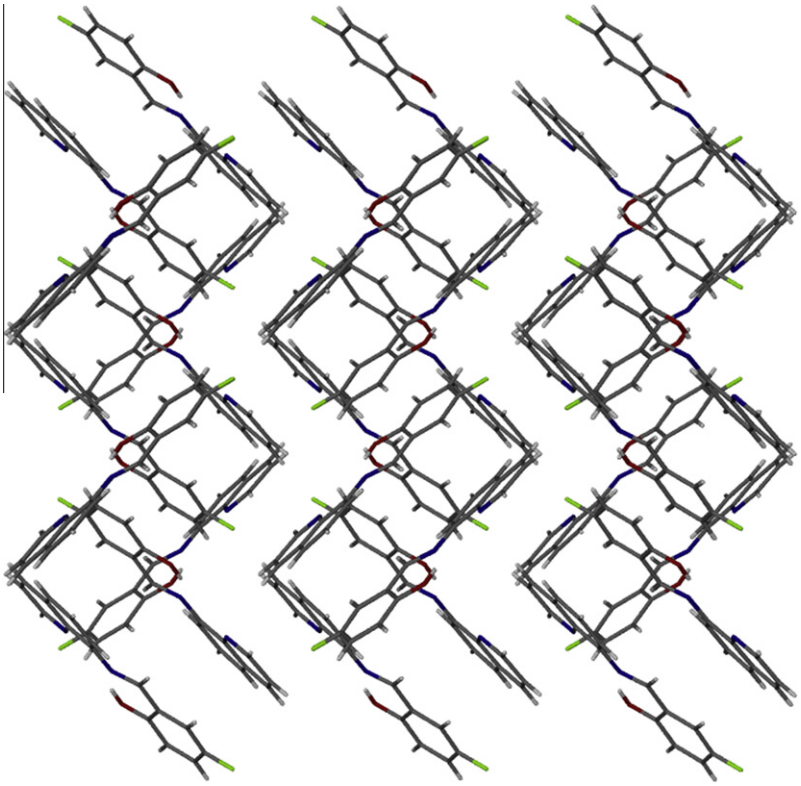

Fig. 5. Rectangular 'tubes' in **1** viewed down the *c* axis.

This is surprising given that studies on the halogen substituted compounds 4-halo-N-(2-fluorophenyl)benzamide reveal that the chloro, bromo and iodo substituted compounds are all isostructural [16]. Similarly, (4-halophenyl)-N-(2-cyanophenyl)methanimine (X = fluoro, chloro, bromo) are also isostructural [18].

A feature of the structures is the presence of a strong hydrogen bond between the phenolic O—H group and the imine nitrogen with O—H···N distances varying from 1.76 to 1.84 Å (see Fig. 1). A similar interaction is also observed in Hqsal although in this case the distance is much shorter, 1.593 Å [29].

The structures also involve stacks of the Hqsal^{X} molecules and in most cases form a herringbone packing pattern. However, it is important to note that the interactions used to form these stacks are not always the same. In quantifying these stacks we have chosen to use two angles θ and ϕ which represent the angle between the quinolyl and salicylaldimine moiety and the angle between neighbouring Hqsal^{X} molecules, respectively (see Fig. 2). Thus, for Hqsal^{X} (X = F, Br and I) the quinoline ring is oriented such that the ligand is preorganized to coordinate a metal atom (see Fig. 1). However, the degree of coplanarity between the two aromatic rings varies from 5.1° in Hqsal^{I} to 22.6° in Hqsal^{Br} (see Table 2).

In contrast with the other structures in this series, in Hqsal^{Cl} the quinoline ring points away from the O—H···N hydrogen bond with the intramolecular angle between the rings 133.7°. A similar observation has been made for Hqsal$^{3\text{-}SiPh3,5\text{-}Me}$, although this is thought to be due to steric effects [31]. For Hqsal^{Cl} the rotation of the quinoline ring allows the formation of a hydrogen bonding square between neighbouring phenolic O—H groups creating a dimer (2.545 Å, see Fig. 3). Interestingly, the related compound 4-chloro-2-(1-naphthyliminomethyl)-phenol where the quinoline ring is replaced by a naphthyl group reveals a normal conformation, i.e. $\theta < 90$ in this case 56.9° [32]. Moreover, the bromo substituted compound 4-bromo-2-(1-naphthylimino-methyl)phenol [33] has essentially an identical

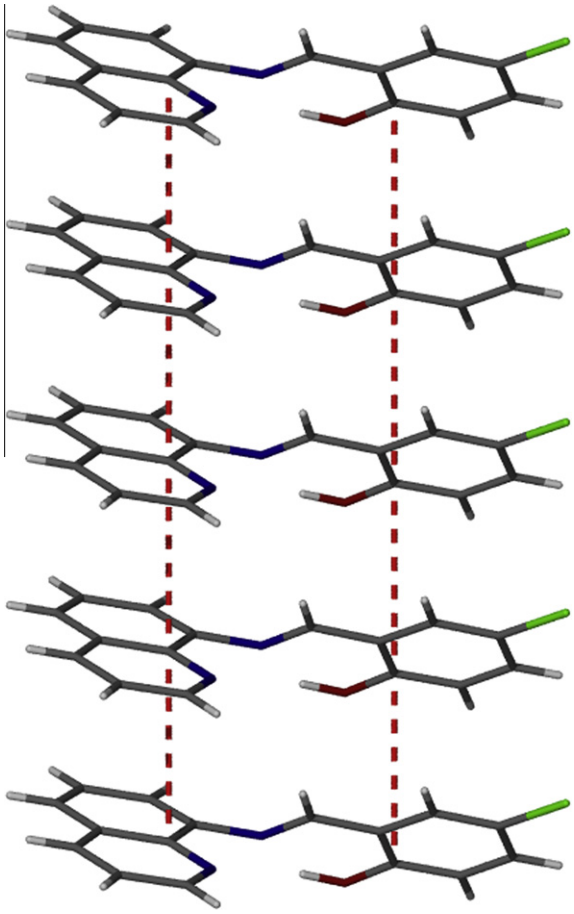

Fig. 6. π–π Interactions showing the 1D pillar in the structure of **2** viewed down the *a* axis.

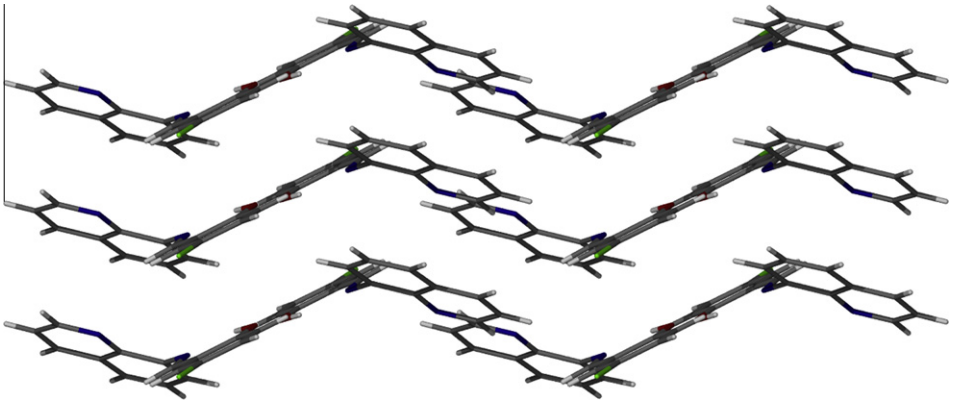

Fig. 7. View of the wave like planes in **2**, viewed down the *c* axis.

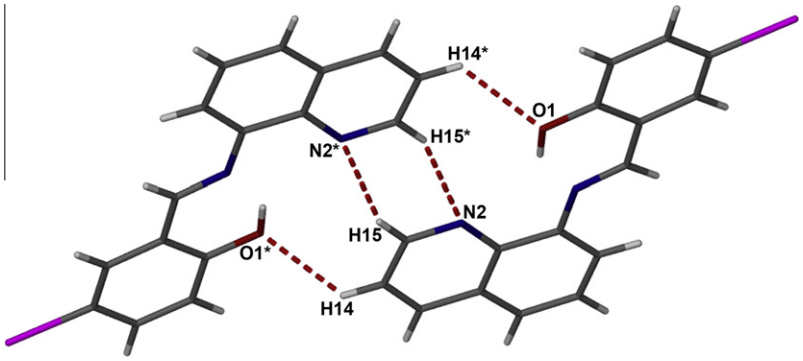

Fig. 8. View of the C—H···N and C—H···O interactions that form the narcissistic dimer in **4** (*symmetry code = 1 − *x*, 1 − *y*, −*z*).

Table 3
Parameters for the interactions in the Hqsal^{X} ligands.

	D—H···A	D—H (Å)	D···A (Å)	H···A (Å)	∠D—H···A (°)	Symmetry
Hqsal^{F} **1**	O(1)—H(1)···N(1)	0.82	2.571(2)	1.843	147	*x*, *y*, *z*
	C(9)—H(9)···O(1)	0.93	3.358(2)	2.536	147	*x*, ½ − *y*, ½ + *z*
Hqsal^{Cl} **2**	O(1)—H(1)···N(1)	0.94	2.589(3)	1.760	146	*x*, *y*, *z*
	O(1)—H(1)···O(1)	0.94	2.926(3)	2.545	105	1 − *x*, −*y*, 2 − *z*
	C(9)—H(9)···O(1)	0.95	3.551(3)	2.694	150	1 − *x*, 1 − *y*, 2 − *z*
Hqsal^{Br} **3**	O(1)—H(1)···N(1)	0.84	2.577(2)	1.832	147	*x*, *y*, *z*
	C(15)—H(15)···N(2)	0.95	3.520(3)	2.660	151	−*x*, −*y*, 1 − *z*
	C(14)—H(14)···O(1)	0.95	3.287(3)	2.706	120	−*x*, −*y*, 1 − *z*
Hqsal^{I} **4**	O(1)—H(1)···N(1)	0.84	2.567(8)	1.823	147	*x*, *y*, *z*
	C(15)—H(15)···N(2)	0.95	3.624(8)	2.732	157	1 − *x*, 1 − *y*, −*z*
	C(14)—H(14)···O(1)	0.95	3.228(9)	2.593	124	1 − *x*, 1 − *y*, −*z*

structure to the chloro derivative in stark contrast to our own findings with **2** and **3**, indicating that the quinoline influences which conformation is preferred.

The angle between the stacks is remarkably similar for **1**, **3** and **4** varying from 81.3° to 89.7° and does not seem to reflect the size of the halogen or the angle, θ. Once again, Hqsal^{Cl} differs from the other members of the series with ϕ 133.7° and identical to θ as the molecule sits at the inflection point of the herringbone packing motif.

The structure of Hqsal^{F} is unique in this series with inversely parallel dimers being formed through weak offset π–π interactions between the phenyl and quinoline rings. Similar dimers are also present in the structure of Hqsal although these are held together by interactions between the C—O and C=N groups [29]. Moreover, here there are additional π–π interactions between the phenyl rings of neighbouring dimers resulting in a 1D stepped chain (Fig. 4).

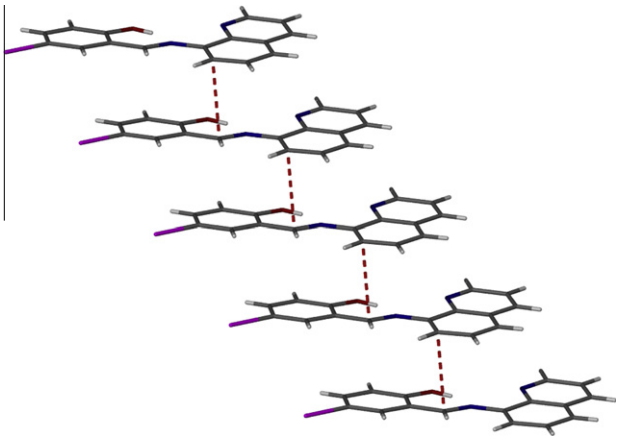

Fig. 9. View of the offset stacks in **4**.

A further stepped chain also composed of π–π stacked dimers is perpendicular to the first chain and connected to it via C—H···O interactions between the phenolic oxygen atom and a C—H group on the quinoline ring (see Fig. S1). Combined these interactions serve to create an extended rectangular 'tube' with identical 'tubes' isolated from each other (Fig. 5).

The structure of Hqsal^{Cl} is composed of 1D pillars formed by π–π interactions between the phenyl and quinoline rings but in contrast to Hqsal [29] and Hqsal^{F} the aromatic rings are located directly on top of one another (Fig. 6). The 1D pillar is then connected to another pillar via the hydrogen bonding square described in Fig. 3. Finally, two types of C—H···π interactions (C5—H5···C14 = 2.858 Å, C14—H14···C5 2.791 Å, Fig. S2) serve to link the pairs of pillars to one another. Similar pillars are found in 4-chloro-2-(1-naphthyliminomethyl)phenol, although these are linked via C—H···O interactions. A perpendicular view of the pillars reveals wave like planes with the Hqsal^{Cl} molecule positioned at the 'peaks' and 'valleys' of the wave (see Fig. 7).

The structures of Hqsal^{Br} and Hqsal^{I} while not isostructural do share many of the same structural motifs and as such will be discussed together. The most important structural motif is the presence of narcissistic dimers formed from two sets of complementary C—H···N and C—H···O interactions between neighbouring hydrogens on the quinoline ring and the quinoline nitrogen and phenolic oxygen, respectively (Fig. 8). However, there is a subtle difference between the two structures such that for Hqsal^{Br} the C—H···N interactions are stronger than the C—H···O interactions while in Hqsal^{I} the situation is reversed (see Table 3). This is due to the greater degree of non-coplanarity in Hqsal^{Br} which places H14 further away from the phenolic oxygen. However, in Hqsal^{I} the coplanarity of the two aromatic rings means that a close contact between the phenolic oxygen and H14 limits the proximity of H15 and N2.

In both compounds the molecules form offset stacks through interactions between the C=N group and the quinoline ring (C7···C9 = 3.175 Å in **3**, C7···C9 = 3.302 Å in **4**, see Fig. 9). The stacks are offset, in part, due to the bulky bromo and iodo substituents which prevent the large degree of overlap found in **1** and **2**. In the case of Hqsal^{I}, there are additional weak N(lone pair)–π interactions (Cg 1···N1 = 3.424 Å, where Cg 1 = C8—C12,C16). A similar interaction is found in the structure of [Cu_2Cl_2(N′-[1-(pyridin-2-yl)ethylidene]acetohydrazide)$_2$] between one of the coordinated nitrogen atoms and the pyridyl ring (Cg···N = 3.421 Å) [34]. Once again the non-coplanar nature of the aromatic rings in Hqsal^{Br} precludes the formation of this interaction. These columns are then connected to neighbouring columns through the narcissistic interaction described in Fig. 8.

The packing in the structure of the two compounds is completed through C—H···π interactions resulting in a fishbone packing pattern (see Fig. 10a). Interestingly while Hqsal^{I} achieves this through a single type of C—H···π interaction (C13—H13···C13 = 2.768 Å, see Fig. S3), **3** employs three separate C—H···π interactions (C13—H13···C3 2.874 Å, C3—H3···C14 2.814 Å, C10—H10···C10 2.875 Å; Fig. 10b) leading to a greater degree of interconnectivity in this structure.

It is interesting to note that in all the structures despite the presence of halogens in these systems none of the halogens are found to be involved either in C—H···X or C—X···X bonding. The reason for this probably relates to the presence of additional interactions, in particular π–π, C—H···N and C—H···O interactions which necessarily limit the formation of halogen bonds. Similar findings are reported in the series 4-halo-N-(fluorophenyl)benzamide [16]. This is somewhat surprising particularly in the case of iodine which is the most polarizable of the halogens and more commonly involved in halogen bonding [13,18]. It is important to note that although the halogens do not engage in halogen bonding they are key in determining which structure is the most favourable. Thus, fluorine which is the smallest member in the series and most electronegative gives rise to a structure with extensive π–π stacking with the Hqsal^{F} inversely parallel. In contrast, the large steric bulk of iodine prohibits such interactions and strongly offset stacks are observed with the Hqsal^{I} now stacked parallel.

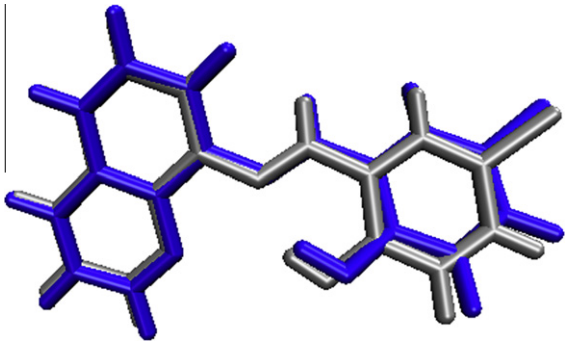

Fig. 11. Overlay of the computed (blue) and molecular structure determined by X-ray diffraction (grey) of Hqsal^{Br} **3**. (For interpretation of the references to colour in this figure legend, the reader is referred to the web version of this article.).

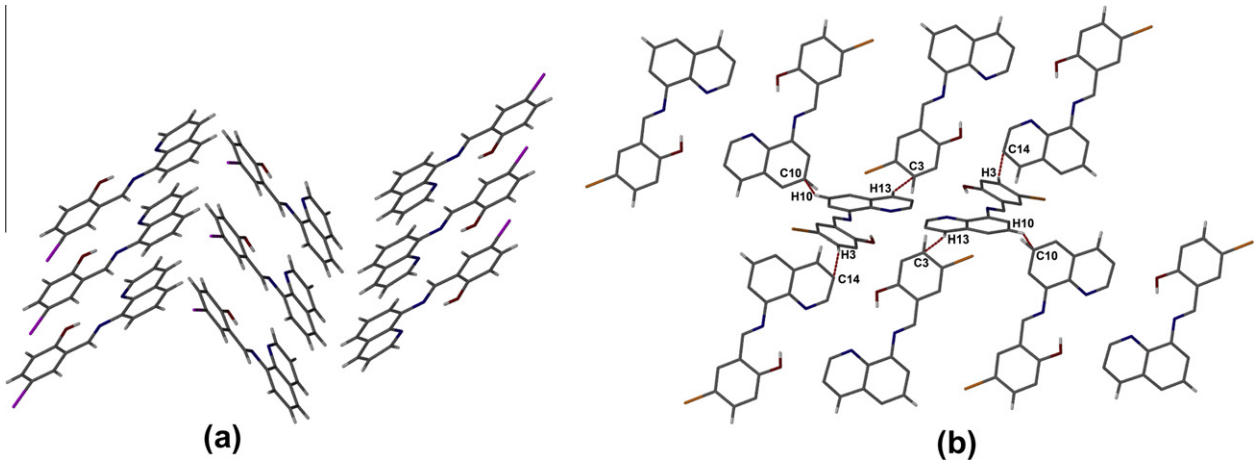

Fig. 10. (a) Fishbone packing in **4** viewed down the *a* axis and (b) C—H···π interactions in **3** viewed down the *b* axis, only hydrogens involved in interactions are shown for clarity.

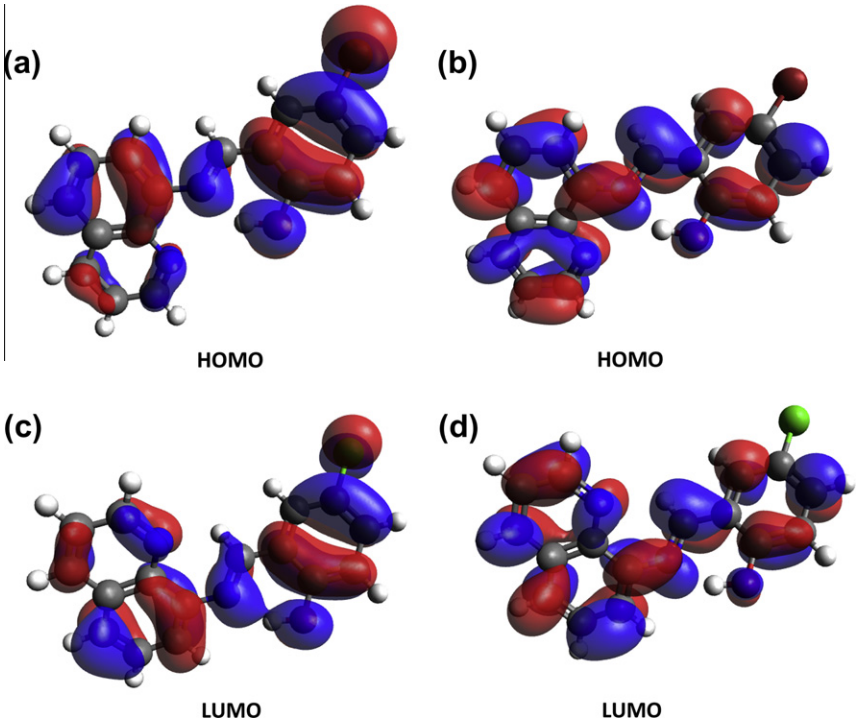

Fig. 12. HOMOs and LUMOs of $Hqsal^{Br}$ (right) and $Hqsal^{Cl}$ (left).

Electronics are clearly important too as evidenced by the structure of $Hqsal^{Cl}$ where an additional O—H···O hydrogen bond forms as a result of the quinoline group being rotated away from the hydroxyl group.

3.3. Computational studies

In order to better understand the conformational preferences for the different halogens and in particular why $Hqsal^{Cl}$ should have the shortest O—H···O hydrogen bond we undertook DFT calculations. The structures were all optimized with the B3LYP calculation using a 6-31G* basis set. Comparison of the optimized structures reveals that the atom–atom bond lengths are in agreement within 0.03 Å and bond angles within 5° indicating that the calculations accurately model the $Hqsal^{X}$ compounds. Further proof of this is evidenced by an overlay of the molecular structure determined by X-ray diffraction of $Hqsal^{Br}$ and its calculated structure (Fig. 11).

Interestingly, the optimized structures of **1**, **3** and **4** show low θ values while **2** displays a large θ value such that the quinoline ring is rotated away from the O—H···N hydrogen bond exactly matching that found in the crystal structure. The inverted conformation found in **2** must therefore be a consequence of the electronic effects of the chloro substituent. Thus, the hydrogen bonding square (see Fig. 3) is a result of the inverted conformation rather than the driving force for it. Moreover, single point calculations for all $Hqsal^{X}$ ligands both in the inverted and normal conformation reveal that in every case the O—H···N hydrogen bond is shorter when the ligand is in an inverted conformation indicating that the shorter hydrogen bond in **2** is due to the inverted conformation.

To provide further insight into the effect of the X group on the structures we also examined the frontier orbitals of the compounds. The compounds are all broadly similar with the salicylaldimine moiety dominating the HOMO. However, the degree of participation of the halogen in the HOMO varies with F contributing the least and I the most. Interestingly, there is orbital overlap between the imine nitrogen and hydroxyl group in the case of $Hqsal^{Cl}$ and consistent with the stronger hydrogen bonding in this compound. In contrast, the LUMOs are essentially identical throughout the series being composed principally of π^* orbitals with slightly more electron density being found on the quinoline. Moreover, there is no electron density on the halogen in the LUMO explaining the comparative similarity of the different $Hqsal^{X}$ LUMOs (see Fig. 12).

4. Conclusions

In conclusion, we have successfully prepared a complete set of halogen substituted quinolylsalicyaldimines. The packing within the structures is dominated by π–π, C—H···N and C—H···O interactions which form stacks although the angle and type of stacks formed and the individual interactions which hold these stacks together vary depending on the halogen. The results clearly demonstrate that both the steric and electronic effects of the halogens need to be considered when attempting to predict what structure will be obtained, although computational studies are able to predict conformational preferences of the *individual* molecules. Moreover, it is evident that introduction of a halogen into a molecule does not guarantee the presence of halogen bonding in the resulting structure and further emphasizes the challenge of trying to predict crystal structures based purely on the molecular structure.

Acknowledgements

We thank the National Science and Technology Development Agency (Grant No.: P-10-11181) for funding this research. We also thank the Development and Promotion of Science and Technology Talents Project for a Ph.D. scholarship (to W.P.) and Walailak University for a Postdoctoral Research Fellowship to J.S. (Grant No.: WU55701). The University of Bristol is thanked for elemental analysis.

Appendix A. Supplementary material

Supplementary data associated with this article can be found, in the online version, at http://dx.doi.org/10.1016/j.molstruc.2012.11.028.

References

[1] D. Braga, G.R. Desiraju, J.S. Miller, A.G. Orpen, S.L. Price, CrystEngComm 4 (2002) 500–509.
[2] K. Biradha, C.-Y. Su, J.J. Vittal, Cryst. Growth Des. 11 (2011) 875–886.
[3] T. Steiner, Angew. Chem., Int. Ed. 41 (2002) 48–76.
[4] G.R. Desiraju, Angew. Chem., Int. Ed. 50 (2011) 52–59.
[5] G.R. Desiraju, Acc. Chem. Res. 35 (2002) 565–573.
[6] M. Khan, V. Enkelmann, G. Brunklaus, Cryst. Growth Des. 9 (2009) 2354–2362.
[7] T.J. Mooibroek, P. Gamez, J. Reedijk, CrystEngComm 10 (2008) 1501–1515.
[8] C. Janiak, Dalton Trans. (2003) 2781–2804.
[9] C.R. Martinez, B.L. Iverson, Chem. Sci. 3 (2012) 2191–2201.
[10] M. Nishio, Y. Umezawa, K. Honda, S. Tsuboyama, H. Suezawa, CrystEngComm 11 (2009) 1757–1788.
[11] S.L. Price, Acc. Chem. Res. 42 (2009) 117–126.
[12] G. Cavallo, P. Metrangolo, T. Pilati, G. Resnati, M. Sansotera, G. Terraneo, Chem. Soc. Rev. 39 (2010) 3772–3783.
[13] P. Metrangolo, F. Meyer, T. Pilati, G. Resnati, G. Terraneo, Angew. Chem., Int. Ed. 47 (2008) 6114–6127.
[14] J.-A. van den Berg, K.R. Seddon, Cryst. Growth Des. 3 (2003) 643–661.
[15] E. Corradi, S.V. Meille, M.T. Messina, P. Metrangolo, G. Resnati, Angew. Chem., Int. Ed. 39 (2000) 1782–1786.
[16] S.K. Nayak, M.K. Reddy, T.N. Guru Row, D. Chopra, Cryst. Growth Des. 11 (2011) 1578–1596.
[17] D. Chopra, Cryst. Growth Des. 12 (2011) 541–546.
[18] W.H. Ojala, K.M. Lystad, T.L. Deal, J.E. Engebretson, J.M. Spude, B. Balidemaj, C.R. Ojala, Cryst. Growth Des. 9 (2009) 964–970.
[19] A.G. Dikundwar, T.N.G. Row, Cryst. Growth Des. 12 (2012) 1713–1716.
[20] T. Clark, M. Hennemann, J. Murray, P. Politzer, J. Mol. Model. 13 (2007) 291–296.
[21] G. Valerio, G. Raos, S.V. Meille, P. Metrangolo, G. Resnati, J. Phys. Chem. A 104 (2000) 1617–1620.
[22] A.M. Donia, H.A. El-Boraey, Transition Met. Chem. 18 (1993) 315–318.
[23] K. Katuki, K. Isagai, Bunseki Kagaku 22 (1973) 1470–1474.
[24] Bruker. Bruker AXS Inc., Madison, Wisconsin, USA, 2005.
[25] Bruker. Bruker AXS Inc., Madison, Wisconsin, USA, 2003.
[26] G.M. Sheldrick, Acta Crystallogr. A64 (2008) 112–122.
[27] L.J. Barbour, J. Supramol. Chem. 1 (2001) 189–191.
[28] J.L. Atwood, L.J. Barbour, Cryst. Growth Des. 3 (2003) 3–8.
[29] J. Wagler, D. Gerlach, G. Roewer, Inorg. Chim. Acta 360 (2007) 1935–1942.
[30] D.J. Harding, D. Sertphon, P. Harding, K.S. Murray, B. Moubaraki, J.D. Cashion, H. Adams, Chem. Eur. J. (2012), http://dx.doi.org/10.1002/chem.201202053.
[31] E. Kirillov, T. Roisnel, A. Razavi, J.-F. Carpentier, Organometallics 28 (2009) 2401–2409.
[32] Z.-X. Li, X.-L. Zhang, Acta Crystallogr. Sect. E 61 (2005) o875–o876.
[33] X.-S. Tai, J. Yin, Y.-M. Feng, Acta Crystallogr. Sect. E 63 (2007) o699–o700.
[34] K. Das, A. Datta, C. Sinha, J.-H. Huang, E. Garribba, C.-S. Hsiao, C.-L. Hsu, ChemistryOpen 1 (2012) 80–89.